Computational Study on the Clamping Mechanism in Injection Molding Machine

Van-Duong Le
Van-Thanh Hoang
Tao Quang Bang (TQBANG@DUT.UDN.VN)
The University of Danang - University of Science and Technology
Lahouari Benabou
Ngoc-Hai Tran
Duc-Binh Luu
Jang Min Park

Research Article

Keywords: Injection molding machine, Clamping mechanism, Optimized parameters, Force amplification, Computational study

Posted Date: March 16th, 2022

DOI: https://doi.org/10.21203/rs.3.rs-1431947/v1

Computational Study on the Clamping Mechanism in Injection Molding Machine

Van-Duong Le[1], Van-Thanh Hoang[1], Quang-Bang Tao[1*], Lahouari Benabou[2], Ngoc-Hai Tran[1], Duc-Binh Luu[1], and Jang Min Park[3*]

[1]Faculty of Mechanical Engineering, The University of Danang - University of Science and Technology, Danang city, 550000, VietNam

[2]LISV, University of Versailles Saint Quentin en Yvelines, University of Paris Saclay, France

[3]School of Mechanical Engineering, Yeungnam University, Daehak-ro 280, Gyeongsan 38541, Republic of Korea

*Corresponding author:

E-mail address: tqbang@dut.udn.vn (Q.B. Tao), jpark@yu.ac.kr (J. M. Park).

Abstract

The clamping mechanism plays an important role in obtaining high-quality products of the injection molding process. The clamping mechanism of five-point double-toggle has been widely used for the high-speed plastics injection molding machine. The purpose of this paper is to optimize the five-point double-toggle clamping mechanism through multi-body dynamics analysis. This work also provides guidelines and a clear understanding for designing the clamping system in an injection molding machine with various clamping forces. The theoretical calculation has been handled first and then the computational model has been verified in this study. In addition, the effects of clamping forces on the main dimensions, including movable-fixed plate thickness, tie-bar diameter and average link cross-section have been investigated theoretically and numerically. The results show that the optimal design allows reaching a high force amplified ratio and that the obtained mechanism has good kinematic performance and works steadily with lower energy consumption and lower cost than the preliminary design. Moreover, the relationships between the parameters such as the critical angles of the double-toggle clamping mechanism, the ratio of force amplification and the stroke of movable mold have been found in this work. The optimized parameters will yield useful knowledge to design and manufacture the clamping mechanism of the micro injection molding machine in practice.

Keywords: Injection molding machine, Clamping mechanism, Optimized parameters, Force amplification, Computational study

1 Introduction

Nowadays, the injection molding process has been widely used for the mass production of complicated geometries with high dimensional precision. Molded part quality largely depends on the accuracy of the injection molding machine and processing parameters as well. The molding clamping system is one of the most crucial systems that directly affects the dimensional accuracy and the quality of the molded products. The clamping unit is used to keep the mold shut against the forces developed when injection pressure pushes melt plastics into the cavity. There have been many studies on the nine-link type mold/die clamping mechanism due to their wide applications in the industry for years. As far as theoretical analysis is concerned, Choubey and Rao approximated kinematic errors more precisely by taking into account both minimizing structural and mechanical errors [1]. For experimental method, there are many studies presented in the literature. For example, Rao et al. [2] and Huang et al. [3, 4] used strain gauge-based sensors to measure the elongation of the tie bar and to further estimate the clamping force. Chang et al. investigated a new design of a tie-bar-less clamping system for micro–injection molding machines [5]. The ultrasonic probes are installed on the ends of the tie bars, to measure the clamping force based on the proposed model relating the ultrasonic propagation time to the clamping force of the mechanism are also carried out by Zhao et al. [6]. With regard to theoretical analysis and experimental solution, a case study was conducted by Chang et al. in order to consider kinematic error equations of links and tolerances in nine-link type double-toggle mold/die clamping mechanisms [7]. Lin et al. explored the friction effects at pin joints of the clamping mechanism during real clamping operation [8]. They also improved the clamping system to enhance performances of stroke ratio and thrust saving as well as design a reasonable space for ejector unit [9, 10]. In other work, there have been different approaches presented based theoretical analysis and simulation. Zhang et al. analyzed a performance of the mold clamping mechanism in injection molding machine by evaluating the microstructure, stress, travel, speed ratio, and the ratio of amplified force. Then the designed clamping mechanism with microstructure is studied by the theoretical analysis and simulation [11]. The genetic algorithm (GA) numerical technique to optimize the key design parameters of the clamping mechanism is adopted by Huang et al. [12]. Fung et al. also investigated

kinematic and sensitivity of a newly designed toggle mechanism formed by two slider-crank mechanisms [13]. Besides, X. Li et al. [14] utilized MATLAB to get the optimized parameters of the clamping mechanism such as stroke ratio, velocity ratio and the amplified force ratio of the micro injection molding machine. Moreover, Jiao et al. studied the clamping characteristics of different types of clamping units thanks to the finite element method of the ABAQUS tool and experiment in order to investigate the clamping uniformity and evaluate the clamping force repeatability precision [15].

In those previous works, most of the approaches are limited to theoretical analysis or/and experimental investigation of the clamping mechanism design. It can be seen that the nine-link mechanism should be described by a multi-body dynamics model for a rigorous analysis prior to manufacturing a real injection molding machine to reduce production costs. In addition, up to our knowledge, one cannot find a complete guideline in the literature to help quickly design the clamping mechanism for a wide range of forces in precise micro-injection molding machines. In this regard, the objective of this work is to design the five-point double-toggle clamping mechanism of a micro-injection molding machine by optimal multi-body dynamics numerical analysis and theoretical verification. Thanks to the results of this analysis, we could have useful design suggestions and more insight for designing the clamping system in an injection molding machine.

2 Overview of the mechanism

2.1 Problem description

The clamping unit plays an important function in closing, opening, and holding the mold in the injection molding process. Noticeably, it also allows preventing molten plastics from going out from the cavities during injection molding. The clamping mechanism must induce a sufficient force up to approximately hundreds or even thousands of tons to hold the mold closed. In general, the toggle mechanism presents the advantages of motion efficiency and energy saving, and thus it is commonly adopted as the clamping mechanism for injection-molding machines [12]. The five-point double-toggle mold-clamping mechanism is the most extensively used for injection molding machines with clamping force between 50 and 500 metric tons due to the ideal kinematic velocity system and the mechanical features [8]. In recent years, injection molding machines having this clamping mechanism with forces of up to 5000 metric tons have

been developed continuously. In this regard, we have selected the five-point double-toggle mold-clamping mechanism for the present investigation. The diagram of transmission and the applied force are shown in Fig. 1.

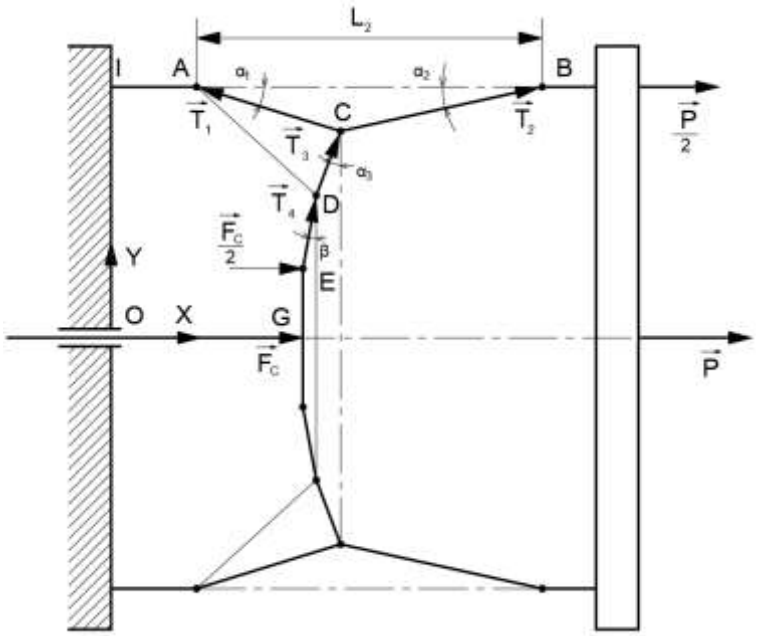

Fig. 1 The five-point double-toggle clamping mechanism of the injection molding machine

A five-point double-toggle clamping mechanism is adopted to exploit the generation of large output clamping force with a small input value of crosshead force. There are nine links of the clamping mechanism such as fixing mold plate, two links *ACD*, two links *BC*, two links *DE*, link cross head, and movable mold plate as shown in Fig. 1. To estimate the multi-body dynamics parameters of the system, relative positions of the links at closed state are defined via angles. The angles α_1, α_2 are formed between the segments *AC*, *BC* and the horizontal line, respectively, and the angles between the segments *CD*, *DE* and the vertical line are α_3, β, respectively. Fig. 2 presents the free body diagram of a five-point double-toggle clamping mechanism. The force $\overrightarrow{F_c}$ induced by the clamping hydraulic cylinder will act on link *DE* via the force $\overrightarrow{T_4}$. The force is transmitted to the link *ACD* and it causes the link *BC* to rotate. At point *C*, there are three forces acting on the point *C*, namely $\overrightarrow{T_1}$, $\overrightarrow{T_2}$ and $\overrightarrow{T_3}$ following the directions of *CA, CB*, and *CD*, respectively. The force $\overrightarrow{T_2}$ allows the movable plate to move to the right for closing the mold. The force

$\vec{P}$ is generated by the toggle mechanism and represents the clamping force of the injection molding machine.

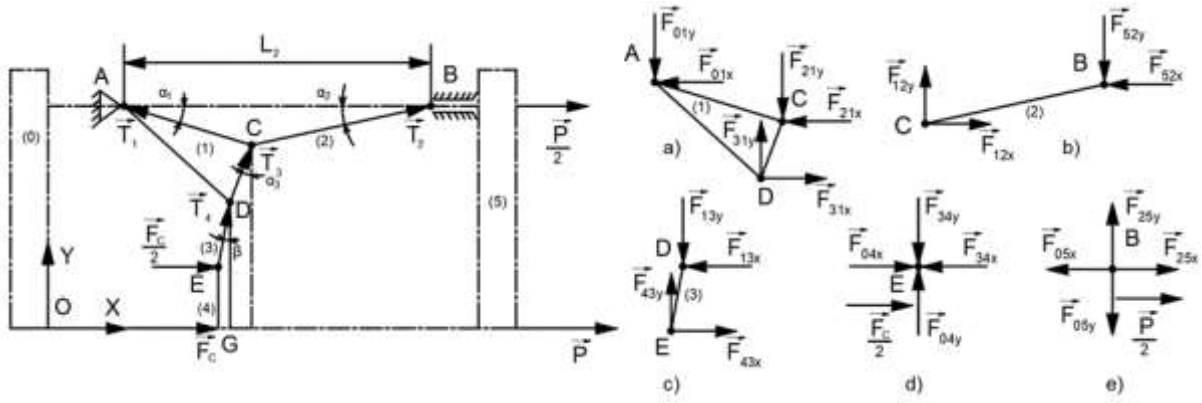

Fig. 2 Free body diagram of the five-point double-toggle clamping mechanism

The force balance equations regarding the free body diagram of the link *ACD* shown in Fig. 2 (a) can be expressed at point *C* as follows:

$$\begin{cases} -F_{01x} - F_{21x} + F_{31x} = 0 \\ -F_{01y} - F_{21y} + F_{31y} = 0 \end{cases} \quad (1)$$

Similarly, the balance of forces acting on the link *DE* shown in Fig. 2(c) are expressed in Eq. (2):

$$-F_{13y} + F_{43y} = 0 \quad (2)$$

At point E, the total force exerted by the crosshead and the link *DE* are shown in Fig. 2(d), and their balance is expressed in Eq. (3):

$$-F_{34x} + F_{04x} = 0 \quad (3)$$

Fig. 2 (e) shows the free-body diagram at point *B* of the link *BC*, where the force balance can be derived in Eq. (4):

$$F_{25x} - F_{05x} = 0 \quad (4)$$

By solving Eqs. (2), (3), (4), the solutions can be expressed as follows: $P = 2T_2 \cos\alpha_2$; $F_c = 2T_4 \sin\beta$; $T_4 = T_3 \frac{\cos\alpha_3}{\cos\beta}$; $T_3 = \frac{T_1 sin\alpha_1 + T_2 sin\alpha_2}{\cos\alpha_3}$; $T_1 = T_2 \frac{cos(\alpha_2+\alpha_3)}{cos(\alpha_1+\alpha_3)}$.

The ratio of force amplification is defined as:

$$K = \frac{P}{F_C} \quad (5)$$

Substituting all force values into Eq. (5), the exact expression for K can be obtained.

$$K = \frac{\cos \alpha_2}{\tan \beta \left(\sin\alpha_2 + \sin\alpha_1 \frac{\cos(\alpha_2 + \alpha_3)}{\cos(\alpha_1 + \alpha_3)} \right)} \quad (6)$$

2.2 Preliminary design

Fig. 3 presents a kinematics diagram of the typical five-point toggle-type clamping unit in injection molding machine, where the system is in a state corresponding to mold closure (the above figure) and mold opening at maximal stroke (the below figure). At the initial design step, the length ratio of the link *AC* to link *CB* is first given the value of 0.8. Applying the geometrical analysis of the clamping mechanism at mold-closing and mold-opening states, the approximately total lengths according to the horizontal direction of the links are obtained by Eqs. (7) and (8) respectively. Therefore, the stroke of the movable mold is 150 mm, which can be expressed by $L_2 - L_1$. The distance between the top link and bottom link can be described by Eq. (9), and the stroke of the hydraulic cylinder and the *IA* length can be defined by Eqs. (10) and (11), respectively.

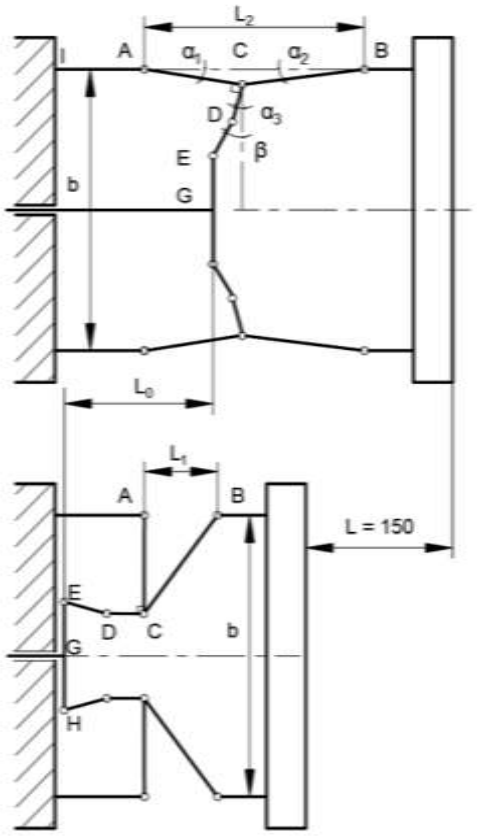

Fig. 3 The diagram to calculate links length of clamping mechanism

$$L_2 = AC\cos\alpha_1 + BC\cos\alpha_2 = BC\,(0{,}8.\cos\alpha_1 + \cos\alpha_2) \quad (7)$$

$$L_1 \approx \sqrt{BC^2 - AC^2} = 0.6BC \quad (8)$$

$$\frac{b}{2} = EG + EDcos(\beta - \alpha_3) + CDcos\alpha_3 + ACsin\alpha_1 \quad (9)$$

$$L_0 = IA + ACcos\ \alpha_1 - CDsin\ \alpha_3 - DEsin(\beta - \alpha_3) \quad (10)$$

$$IA = CD + DEcos(\beta - \alpha_3\ ) \quad (11)$$

The preliminary parameters are taken into account such as the initial angles $\alpha_1 = \alpha_3 = 4°$; $\alpha_2 = 0.8.\alpha_1 = 3.2°$; $\beta = 15.5°$, the crosshead length of 110 mm; *EG* = 55 mm, *CD* = 38 mm, and *b* = 286 mm (*b* > *2AC*). Substituting the values of the initial angles into Eq. (6), the ratio of force amplification is calculated as $K \approx 28.6$. By solving Eqs. (7), (8), (9), (10) and (11), the lengths of the links are obtained: *BC* = 125.3 mm, *AC* = 100.3 mm, *ED* = 45 mm, L_0 = 170 mm; and *IA* = 82 mm. To ensure enough space for connecting the rod of the cylinder to the crosshead, we chose eventually L_0 = 200 mm, and *IA* = 112 mm. From the parameters above, a full 3D model of the clamping mechanism system has been designed as shown in Fig. 4.

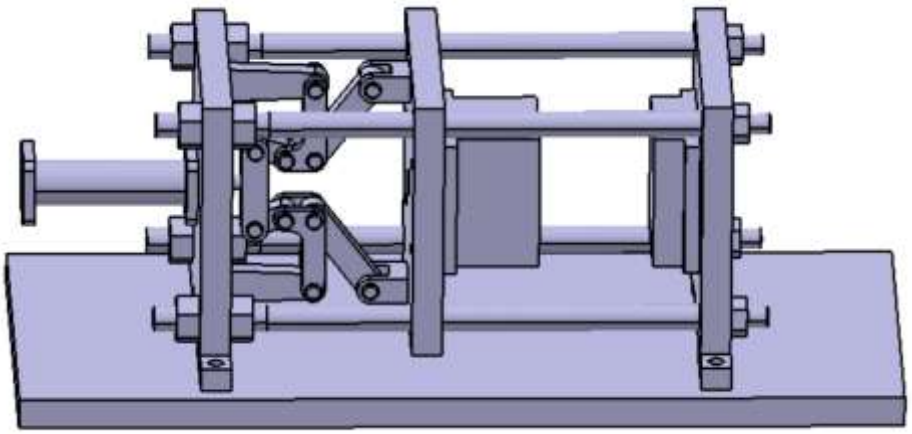

Fig. 4 The full 3D preliminary design of the clamping mechanism

3 Computational model

3.1 Preliminary dynamics analysis

Nowadays, with the strong development of computer sciences, the finite element method is known as one of the most helpful numerical techniques used in the design process thanks to complex calculation and detailed analysis with improved accuracy and reduced computing time [11, 15]. In the present study, software of HyperWorks with

modules of MotionView and HyperStudy were simultaneously used to simulate the clamping mechanism and perform its optimization under multibody dynamics.

As far as the tool MotionView is applied, the procedure can be described by the following steps. Firstly, the linking points of the structure were created by providing the coordinate points. The latter are obtained from 3D CAD software and are used to design the initial structure. Secondly, the 3D data was imported in order to build the links and then applying the materials for these parts were set up. Thirdly, the joints of the clamping system were produced to connect the different links. Then, the imposed motions and driving force were applied as boundary and loading conditions. Finally, the output parameters such as forces in the links and angles were established before moving on to the run analysis. The force at the hydraulic piston is controlled automatically to create the motion of the structure when the position of the link *ACD* reaches critical value in terms of angular position.

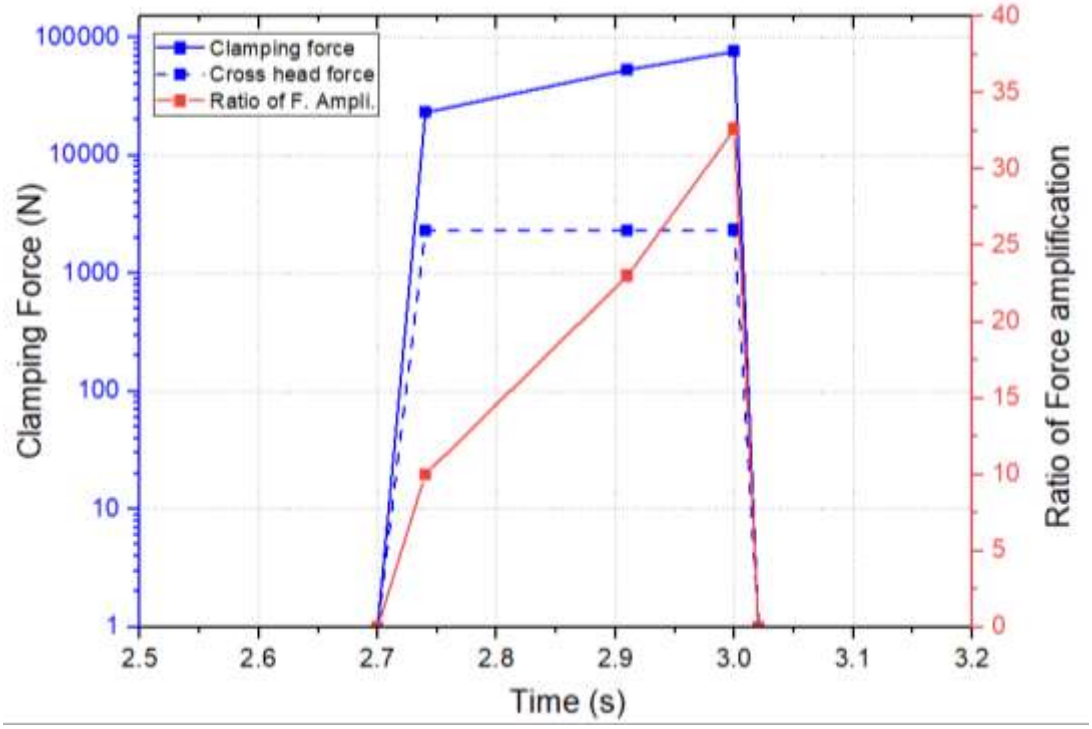

Fig. 5 The diagram of clamping force and K ratio according to dynamics simulation

The results of the initial dynamics simulation of clamping force and ratio of force amplification are shown in Fig. 5. It can be seen that the ratio of force amplification is around 32.6 which shows a good agreement with the theoretical calculation of 28.6. This result is relatively accurate and it can thus be established that boundary conditions and

simulation data set are reasonable. The ratio of force amplification largely depends on the angles α_1, α_2, α_3 and β, which means that the clamping force begins to strongly increase when the mold plates contact each other. The smaller values of these angle lead to the larger values of the ratio of force amplification in the clamping mechanism.

3.2 Establishing optimized modeling on HyperStudy

Optimizing the key parameters of the clamping unit such as the length of links, the initial angle's values α_1, α_2, α_3 and β is extremely important, because this allows to design the toggle mechanism with efficient motion and energy saving when operated [12, 14, 15]. In this study, a new solution by combining the modules of MotionView for dynamics simulation and HyperStudy for digital graph analysis has been applied in order to find the optimized parameters of the clamping mechanism.

For the computational model on HyperStudy, the coordinate equations are employed to defined the relative position of these variables. According to the geometric description shown in Fig. 3, the coordinate equations at points *A, B, C, D, E* can be expressed by Eqs. (12), (13), (14), (15), and (16), respectively.

$$\begin{cases} x_A = IA \\ y_A = \frac{b}{2} \end{cases} \tag{12}$$

$$\begin{cases} x_B = IA + AC.\cos\alpha_1 + BC.\cos\alpha_2 \\ y_B = \frac{b}{2} - AC.\sin\alpha_1 + BC.\sin\alpha_2 \end{cases} \tag{13}$$

$$\begin{cases} x_C = IA + AC.\cos\alpha_1 \\ y_C = \frac{b}{2} - AC.\sin\alpha_1 \end{cases} \tag{14}$$

$$\begin{cases} x_D = IA + AC.\cos\alpha_1 - CD.\sin\alpha_3 \\ y_D = \frac{b}{2} - AC.\sin\alpha_1 - CD.\cos\alpha_3 \end{cases} \tag{15}$$

$$\begin{cases} x_E = IA + AC.\cos\alpha_1 - CD.\sin\alpha_3 - DE.\sin\beta \\ y_E = \frac{b}{2} - AC.\sin\alpha_1 - CD.\cos\alpha_3 - DE.\cos\beta \end{cases} \tag{16}$$

In the computational model, the two points *A, B* are fixed, and there are four variables used in the mold closing state resolution, including the length of *CD*, the length of *DE*, the angle α_3, and the angle β. In this work, these variables are limited with the upper and lower values selected as $32 \le CD \le 46$ (mm), $35 \le DE \le 55$ (mm), $0 \le \alpha_3 \le 16$ (°), and $0 \le \beta \le 16$ (°). The travel distance of the movable mold plate used is 150 mm.

The optimal angles α_1, α_2 are defined through the position of point *C*. Finally, the problem is solved simultaneously by MotionView and HyperStudy integration. In HyperStudy, the data are taken from the dynamics simulation results on MotionView and then it is analyzed according to iteration statement.

3.3 Cross-section of the clamping mechanism according to the optimal results.

The main dimensions of the clamping unit were introduced in the present study such as the cross-section of links, the diameter of the tie bars and the thickness of the plates. The links are subjected to compressive forces when the system is operated, so its strength condition is calculated by Eq. (17), where $[\sigma_n]$ is admissible compressive stress of the material, *A* is the cross-section area of link and *T* is the internal force value of the link. It can be realized that the link *BC* has the maximum internal force T_2, so this link is taken into account for strength analysis. As far as tie bars are concerned in the closing mold state, they are affected by a tension force, the equation for strength condition is obtained by Eq. (18), where $[\sigma_k]$ is the admissible tensile stress of materials; A_c is the cross-sections area of tie–bar. In addition, when the mechanism reaches the maximum clamping force, the moment of deflection caused on the movable mold plate is the largest. Therefore, the thickness of all plates will be computed according to the dimension of the movable mold plate. The size of the movable mold plate is 350 mm x 350 mm, and the hole at the plate center is 60 mm. The strength condition of the plate is defined by Eq. (19), where $[\sigma_b]$ is the admissible tensile strength of the material, W_x is section modulus, M_{max} is the maximal moment of deflection on the plate and the cross section of the plate is *b x h*, in which *b* and *h* are the width and the thickness of plate, respectively.

$$\Sigma A_{cross\ links} \geq \frac{\Sigma T}{[\sigma_n]} \tag{17}$$

$$\Sigma A_{tie\ bar} \geq \frac{P}{[\sigma_k]} \tag{18}$$

$$W_x \geq \frac{|M_{max}|}{[\sigma_b]} \quad ; \quad W_x = \frac{bh^2}{6} \tag{19}$$

3.4 Mesh convergence tests

A mesh study is carried out with computational domain of plate shape in the present study. The beam has cross section of 150 x 30 mm and length of 300 mm and two supports

are applied at the ends of the beam. In addition, a distributed load of 120.000 N over 240 mm length is applied on the beam as shown in Fig. 6. The computational domain discretization was chosen to be done with 5 x 5 x 5 uniform hexahedral elements after preliminary mesh convergence study by using eight types of mesh, namely 15 x 15 x 15, 10 x 10 x 10, 6 x 6 x 6, 5 x 5 x 5, 3 x 3 x 3, 2 x 2 x 2, 1.5 x 1.5 x 1.5, and 1 x 1 x 1. In the mesh convergence test, the simulation results have been examined in terms of stress, and the solution with the mesh of 5 x 5 x 5 is found to be reliable providing almost converged solution with a reasonable computation time under available resources. The mesh ratio is defined by ratio of mesh size to beam thickness as shown in Fig. 7.

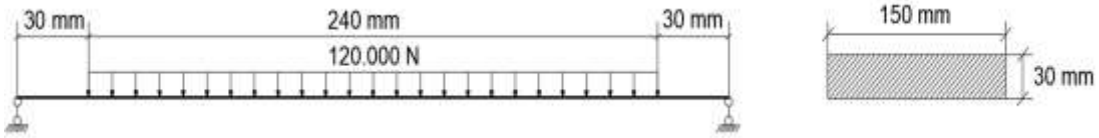

Fig. 6 The convergence tests model

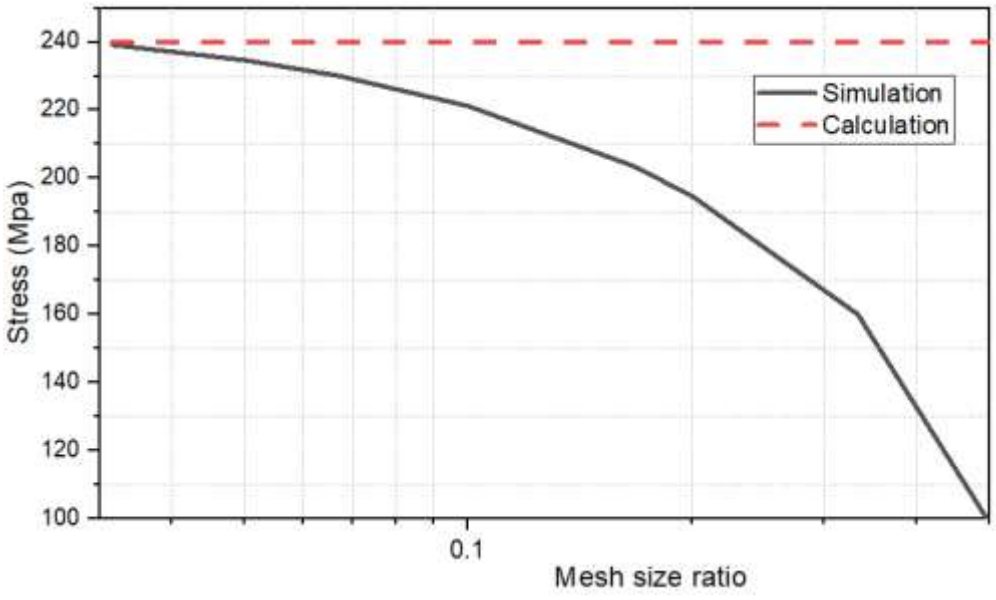

Fig. 7 Results of the mesh size influence study on the stress

3.5 FEM model for durability simulation of the clamping mechanism

In this study, the software HyperWorks [17] with modules of Hypermesh and Optistruct is used for durability simulation. All components of the clamping mechanism are set at the closing mold state. After meshing, the connections between the parts such as bolt and nut, rotary pin and welding joint are created by connectors.

As boundary conditions, the impact force on the movable mold and the reaction force on the fixing mold taken both equal to 30 tons. The force applied at the molds are distributed over the entire contact area between the movable and fixing molds. The problem is solved with the linear static state of Inertia Relief Analysis module in Optistruct. When solving the static problem, finite element solvers will handle the Eq. (20), where *[M]* is the global stiffness matrix, *x* is the displacement vector response and the external forces vector applied to the structure is defined as *f*.

$$f = [M].x \tag{20}$$

4 Results and Discussion

4.1 The optimized designed clamping unit

With the computational model set up above, the value of the optimal parameters obtained by simulation as follows: α_1 = 3.2°; α_2 = 2.55°; α_3 = 13.8°; β = 4.2°; *CD* = 36 mm; *DE* = 45 mm; *EG* = 57.5 mm, and the ratio of force amplification is 129.4, where the input parameters included the maximal clamping force of 30 tons, the plate thickness of 30mm, the cross sections area of links of 9 cm^2, and the tie-bar diameter of 28 mm. The description of the clamping force and the ratio of force amplification as a function of time is plotted in Fig. 8 and Fig. 9.

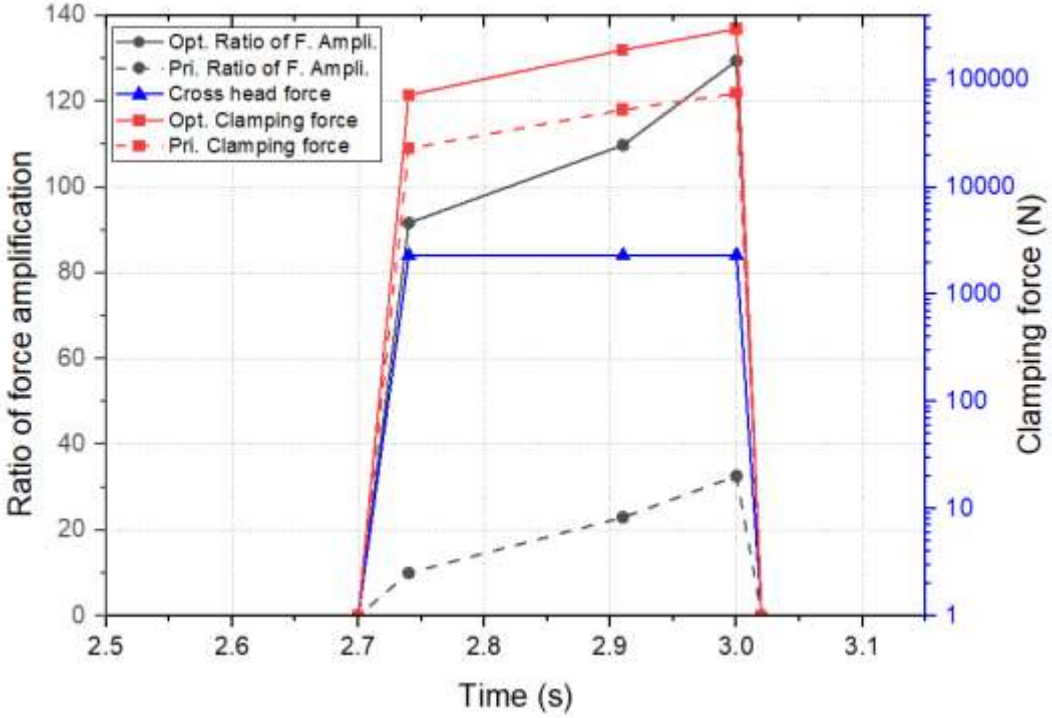

Fig. 8 The optimal ratio of force amplification and clamping force

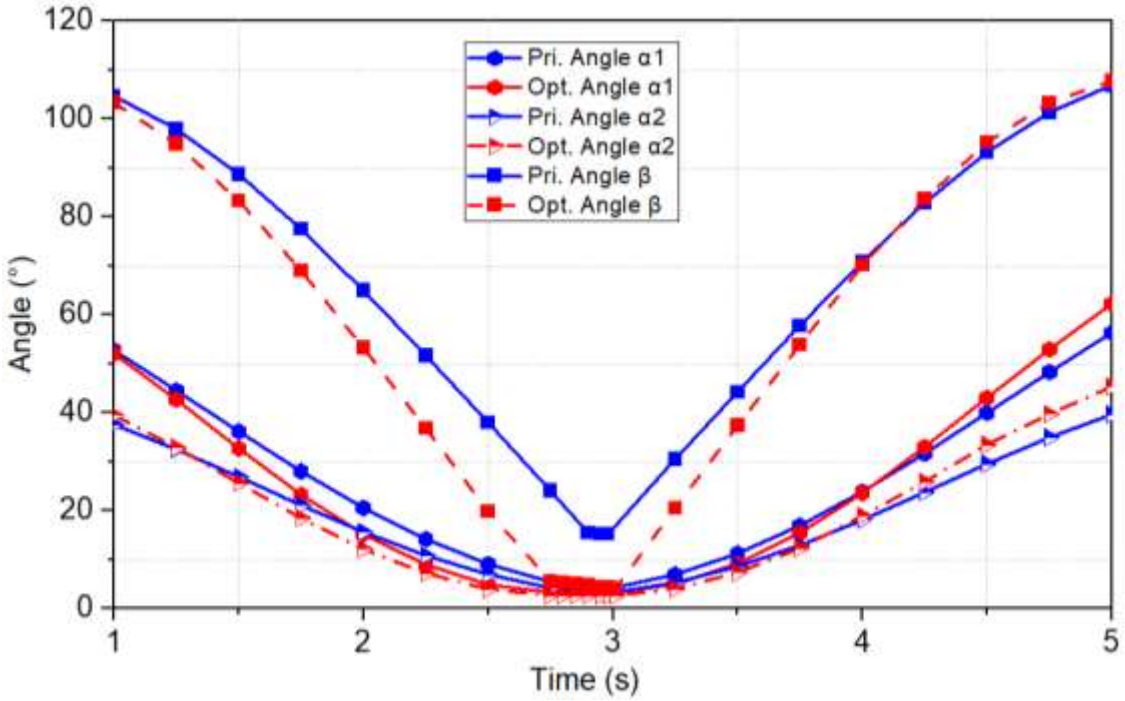

Fig. 9 The value of angle preliminary and optimization

In Fig. 8, it can be noticed that the clamping force is much larger after the optimization, and the clamping force increase with time. The increase up to 30 tons occurs as the movable mold starts to contact with the fixed mold. The optimal value of the ratio of force amplification is four time larger than that of the preliminary design. This high value is of force amplification ratio, means that the mechanism has good kinematic performance, works steadily, generates low energy consumption and has low cost.

Fig. 9 describes the effects of the link angle according to time. In general, the optimal angle values are smaller than the preliminary angle ones. However, the beta angle shows a big difference between the optimal value and the preliminary one. The critical angle values match well with the previous studies handled by Matlab simulation [14, 16], with the alpha critical values of 3.32^{o} and 3.193^{o}, respectively.

Fig. 10 shows the relationship between the link angles and the ratio of force amplification. The clamping force strongly increases when the angles move towards the critical values. The simulation results show a very good agreement with the theoretical calculation, especially for alpha 1 and alpha 2. However, there is a small difference of 4.8 percent between the simulation data and theoretical calculation one. In addition, the angles alpha 1 and alpha 2 represent the significant impact on the ratio of force amplification in comparison with the beta angle. It can be concluded that determining

the optimal critical angle will create a large clamping force and this is known as an advantage for the toggle clamping mechanism.

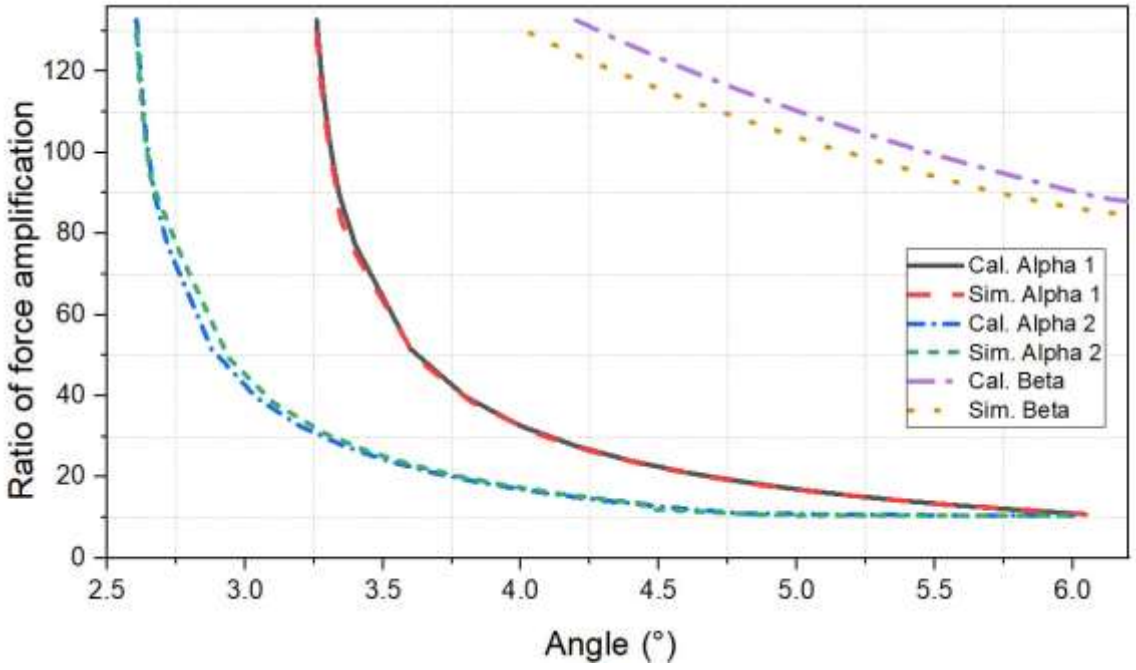

Fig. 10 The relationship between the ratio of force amplification and the initial angles of the links

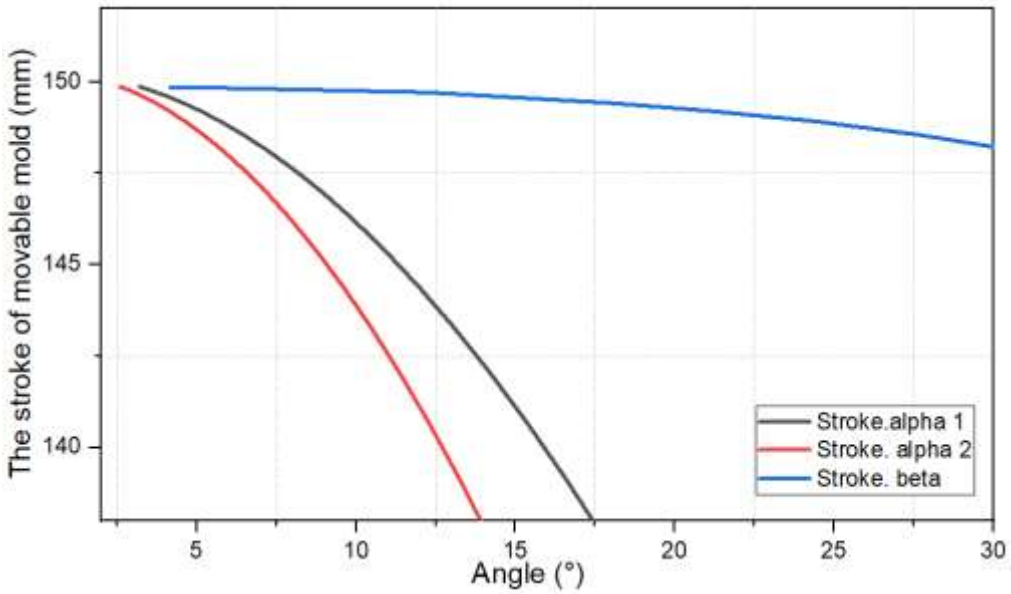

Fig. 11 Relationship between the angles and the stroke of the movable mold

The relationship between the travel distance and the toggle mechanism angles is presented in Fig. 11. The graph shows that effects of angle beta on the stroke of the movable mold plate is much smaller than that of alpha 1 and alpha 2. Furthermore, when

the angles move to the critical values, the rate of movement is slower. This indicates that the optimal mechanism system works smoothly and stably.

4.2 The testing durability of the clamping unit

The relationship between the clamping forces ranging from 10 tons to 50 tons and the main dimensions such as the movable mold plate thickness, the diameter of tie bar and the average cross section of the links are shown in Fig. 12. The stresses used for the theoretical calculation and numerical simulation in comparing with admissible stresses is around 2.5 percent difference and permeable safety factor is not introduced for the study. Obviously, the main dimension increases with the clamping forces. The differences between the theoretical calculation and simulation of the movable mold plate thickness, the tie-bar diameter and the average links cross-section are 4.4%, 1.7%, and 11.8%, respectively. In general, the clamping forces are linearly proportional to the average links cross-sections, whereas the they have been found to be non-linear with the movable mold plate thickness and the tie-bar diameter for smaller clamping forces. The detailed values of the main dimensions corresponding to the clamping forces are presented in Fig. 12.

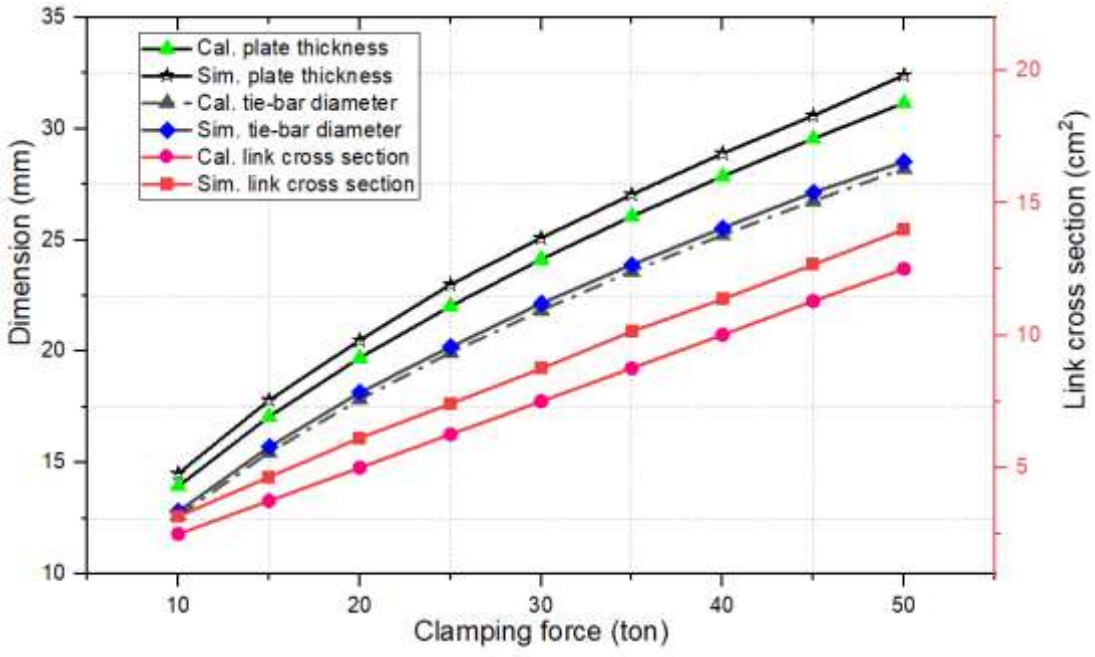

Fig. 12 Relationship between the clamping force and main dimensions of clamping unit

To have a visual insight, Figs. 13-16 provide simulation results of stress which occurs at key joints of the clamping mechanism system at closing mold state. In this study, the main components are designed with safety factor ranging from 1.13 to 1.77. Fig. 13

entirely visualizes the stresses on the clamping unit where maximum stress of 336.6 MPa happens at the junctions between the plate and the links. Fig. 14 shows a clear visualization of the maximum stress of 328.7 MPa on the tie bar where it connects to the fixing plate. Additionally, the maximum stress of 249.4 MPa on the links occurs near the joint with the movable mold plate as shown in Fig. 15. Regarding the movable mold plate, the maximum stress of 293.1 MPa appears around the hole as indicated in Fig. 16.

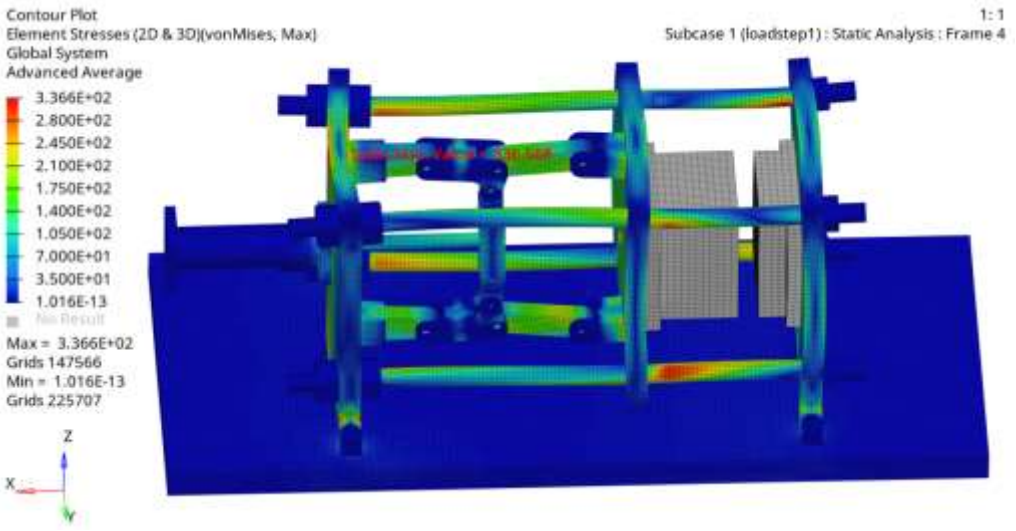

Fig. 13 The stress on the clamping unit in the closing mold state

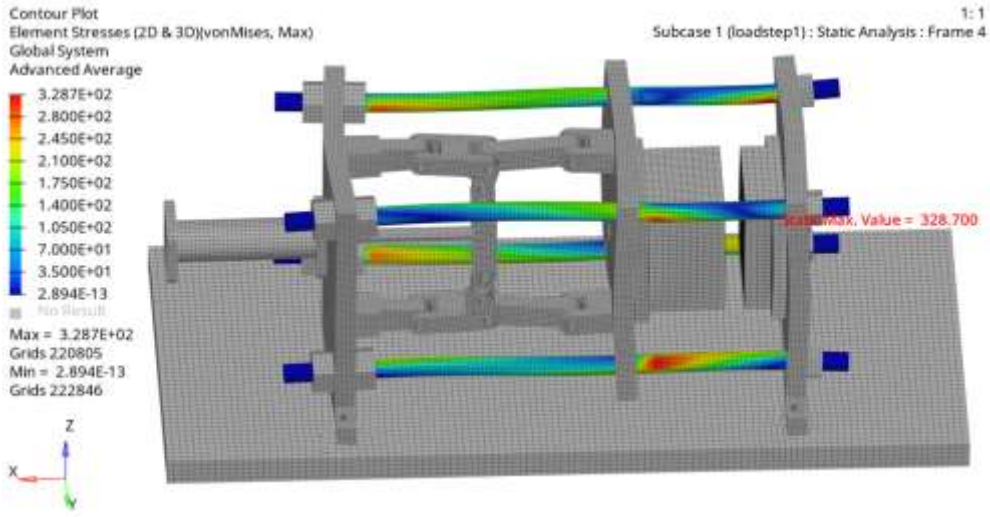

Fig. 14 The stress on tie bar of the clamping unit in the closing mold state

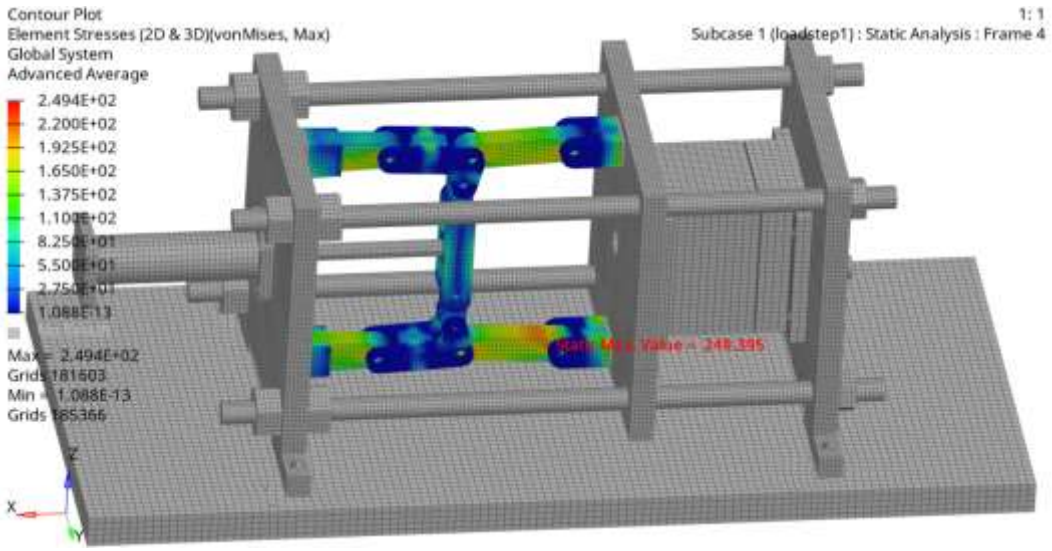

Fig. 15 The stress on links of the clamping unit in the closing mold state

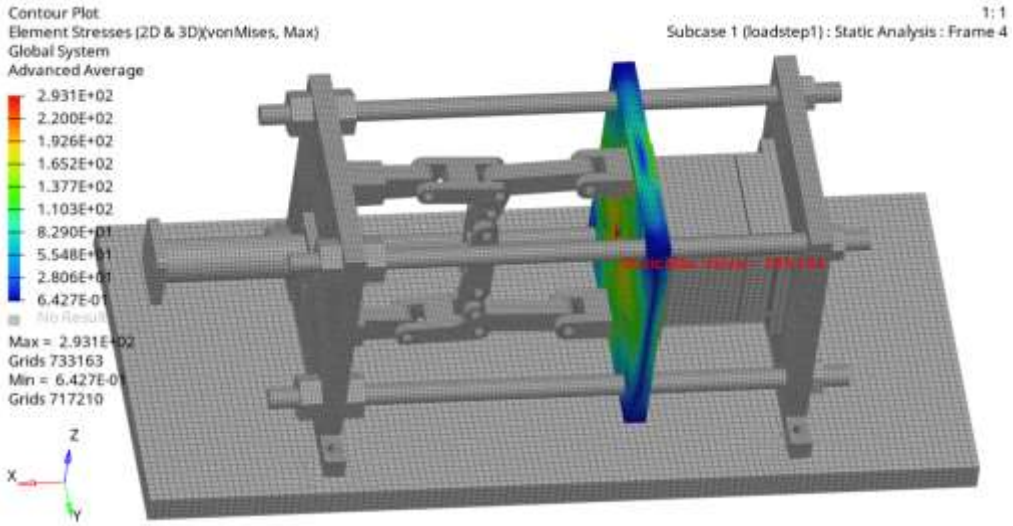

Fig. 16 The stress on movable plate of the clamping unit in the closing mold state

4.3 The prototype fabrication of injection molding machine and molded product

A complete 3D design model of injection molding machine has been built as shown in Fig. 17 (a), where the clamping system is used with a force of 30 tons. An injection molding machine also has been manufactured successfully with the parameters found above as shown in Fig. 17 (b). Initially, the machine worked well during the testing process, and some of its characteristics have been measured to assess its performance such as the stiffness of the structure, its kinematic and stability. In addition, Fig. 18 depicts a prototype article of TIR optical element molded by the injection molding machine designed in the present study.

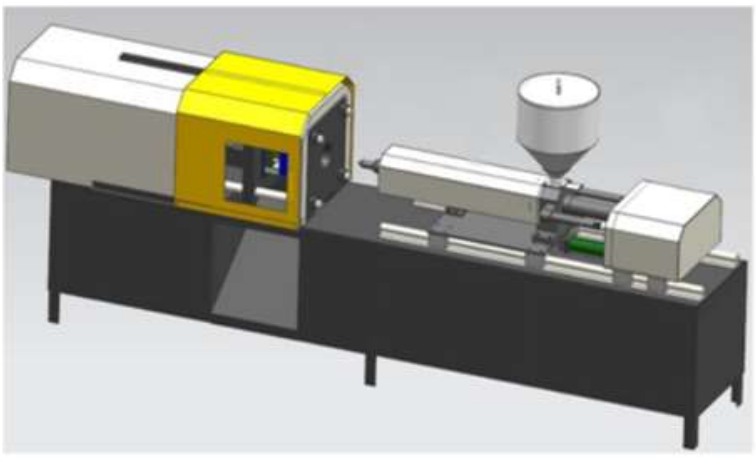

(a)

(b)

Fig. 17 (a) A full 3D design of the machine (b) The injection molding machine fully manufactured

Fig. 18 Sample product fabricated by the designed machine

5 Conclusion

This study has presented the optimal design of the five-point double-toggle mold clamping mechanism in injection molding machine thanks to theoretical and numerical analysis. The effects of the critical angles of the double-toggle clamping mechanism, the ratio of force amplification, and the stroke of the movable mold have been introduced in this paper. In addition, the design parameters, including the movable-fixed plate thickness, the tie-bar diameter and the average link cross-section depending on various clamping forces are taken into account. The theoretical calculation has been found to agree well with the simulation results. Meanwhile, there are some other findings from the present study. Firstly, influence of the alpha 1 and alpha 2 on the ratio of force amplification and the stroke of the movable mold is much larger than that of the beta when the angle tends to zero. Secondly, the cross-section dimension of the link is proportional to the clamping forces. Furthermore, there are many simulation results which show the maximum stresses occurring at the movable-fixed plate, the tie-bar, and the links.

Nomenclatures

Sign	Definition
(0)	fixed mold plate
(1)	link *ACD*
(2)	link *BC*
(3)	link *DE*
(4)	crosshead of the piston
(5)	movable mold plate jointed to the link *BC*
AC	*AC* length of link *ACD*
CD	*CD* length of link *ACD*
IA	the length of the part connecting between the *ACD* link to fixing plate
BC	the length of the *BC* link
EG	the half-length of the link crosshead
α_1	the angle between *AC* and horizontal axis at closing mold
α_2	the angle between *BC* and horizontal axis at closing mold
α_3	the angle between *CD* and vertical axis at closing mold
β	the angle between *DE* and vertical axis at closing mold
F_c	the force of the hydraulic cylinder

P	the clamping force of the machine
F_{ijx}	the force induced from link i acting on link j with the horizontal direction
F_{ijy}	the force induced from link i acting on link j with the vertical direction
b	the vertical distance between two supports IA
L	the stroke of the movable mold plate
L_0	the stroke of the piston
L_2	the length of toggle at closing mold
L_1	the length of toggle at opening the mold
T_1	the force on link ACD with AC direction
T_3	the force on link ACD with CD direction
T_2	the force on the link BC
T_4	the force on the link DE

Funding

This work was supported by The University of Danang, University of Science and Technology, code number of Project: T2022-02-01.

Conflicts of interest

The authors declare that they have no known competing financial interests or personal relationships that could have appeared to influence the work reported in this paper

Availability of data and material: Not applicable

Code availability: Not applicable

Ethics approval: Not applicable

Consent to participate: Not applicable

Consent for publication: Not applicable

Author's contributions

Van-Duong Le performed the calculation and the simulation data, and drafted the manuscript

Van-Thanh Hoang contributed to the design, implementation of the research, and to the writing of the manuscript

Quang-Bang Tao contributed to the analysis of the results and to the writing of the manuscript

Lahouari Benabou contributed to the rewriting of the manuscript and aided in interpreting the results

Ngoc-Hai Tran and Duc-Binh Luu processed the numerical analysis data

Jang Min Park contributed to the re-analysis of the results and to the rewriting of the manuscript.

Van-Duong Le and Van-Thanh Hoang contributed equally to this work. All authors discussed the results and commented on the manuscript.

References

[1] Choubey, M., & Rao, A. C. (1982). Synthesizing linkages with minimal structural and mechanical error based upon tolerance allocation. Mech Mach Theory 17(2): 91-97. https://doi.org/10.1016/0094-114X(82)90039-8

[2] Rao, B., Zhou, H., Ouyang, H., Wan, Y., Zhang, Y., & Wu, J. (2017). Study on the clamping force measurement and partial load regulation technology of injection molding machine. CIRP J Manuf Sci Technol 19: 19-24. https://doi.org/10.1016/j.cirpj.2017.03.001

[3] Huang, M. S., & Lin, C. Y. (2017). A novel clamping force searching method based on sensing tie-bar elongation for injection molding. Int J Heat Mass Tran 109: 223-230. https://doi.org/10.1016/j.ijheatmasstransfer.2017.02.004

[4] Huang, M. S., Nian, S. C., Chen, J. Y., & Lin, C. Y. (2018). Influence of clamping force on tie-bar elongation, mold separation, and part dimensions in injection molding. Precis Eng 51: 647-658. https://doi.org/10.1016/j.precisioneng.2017.11.007

[5] Chang, P. C., Hwang, S. J., Lee, H. H., & Huang, D. Y. (2006). Design and verification of a clamping system for micro-injection molding machine. Trans Can Soc Mech Eng 30(3): 413-428. https://doi.org/10.1139/tcsme-2006-0026

[6] Zhao, Y., Zhao, P., Zhang, J., Huang, J., Xia, N., & Fu, J. (2019). On-line measurement of clamping force for injection molding machine using ultrasonic technology. Ultrasonics 91: 170-179. https://doi.org/10.1016/j.ultras.2018.08.013

[7] Chang, W. T., Lee, W. I., & Hsu, K. L. (2021). Analysis and Experimental Verification of Mechanical Errors in Nine-Link Type Double-Toggle Mold/Die Clamping Mechanisms. Appl Sci 11(2): 832. https://doi.org/10.3390/app11020832

[8] Lin, W. Y., & Hsiao, K. M. (2003). Investigation of the friction effect at pin joints for the five-point double-toggle clamping mechanisms of injection molding machines. Int J Mech 45(11): 1913-1927. https://doi.org/10.1016/j.ijmecsci.2003.10.010

[9] Lin, W. Y., & Hsiao, K. M. (2004). Study on improvements of the five-point double-toggle mould clamping mechanism. Proc Inst Mech Eng C- J Mech 218(7): 761-774. https://doi.org/10.1243/0954406041319482

[10] Lin, W. Y., Shen, C. L., & Hsiao, K. M. (2006). A case study of the five-point double-toggle mould clamping mechanism. Proc Inst Mech Eng C- J Mech 220(4): 527-535. https://doi.org/10.1243/09544062JMES216

[11] Zhang, Y., Wang, X., Williams, J., Huang, Z., Falkner, D., Zhou, G., Yang, Y., Dong, L., Jin, Z., Zhuang, J., Wang, Z., & Liu, Z. (2017). Micro Structure of Injection Molding Machine Mold Clamping Mechanism: Design and Motion Simulation. CAAI Trans Intell Technol 2(3): 157-166. https://pubmed.ncbi.nlm.nih.gov/30272044

[12] Huang, M. S., Lin, T. Y., & Fung, R. F. (2011). Key design parameters and optimal design of a five-point double-toggle clamping mechanism. Appl Math Model 35(9): 4304-4320. https://doi.org/10.1016/j.apm.2011.03.001

[13] Fung, R. F., Hwang, C. C., & Huang, C. S. (1997). Kinematic and sensitivity analyses of a new type toggle mechanism. Jpn Soc Mech Eng Ser C 40(2): 360-365. https://doi.org/10.1299/jsmec.40.360

[14] Li, X., Jin, Z., Zhang, Y., Zhuang, J., Zhou, G., & Wang, L. (2012). Kinematic calculation analysis of micro injection molding machine with double-toggle clamping mechanism based on MATLAB. EMEIT 2012: 1746-1750. https://doi.org/10.2991/emeit.2012.387

[15] Jiao, Z., Liu, H., Xie, P., & Yang, W. (2015). Clamping characteristics study on different types of clamping unit. AIP Conf Proc 1664(1): 110009. https://doi.org/10.1063/1.4918484

[16] Chou, B. G., Cai, H. Z., Zhou, G., Zhang, Y. J., & Zhuang, J. (2014). Design and motion simulation of the clamping mechanism of micro-structure injection molding machine. Adv Mat Res 945: 670-675. https://doi.org/10.4028/www.scientific.net/AMR.945-949.670

[17] Altair HyperWorks Student Edition License